Half-life of ^{44}Ti

D. Frekers, W. Henning, W. Kutschera, K. E. Rehm, R. K. Smither, and J. L. Yntema
Argonne National Laboratory, Argonne, Illinois 60439

R. Santo
Institut für Kernphysik, Universität Münster, D-4400 Münster, Federal Republic of Germany

B. Stievano
Istituto Nazionale di Fisica Nucleare, I-35020 Legnaro, Italy

N. Trautmann
Institut für Kernchemie, Universität Mainz, D-6500 Mainz, Federal Republic of Germany
(Received 26 May 1983)

The half-life of ^{44}Ti has been measured to be $T_{1/2}=54.2\pm2.1$ yr, somewhat higher than previously published values of 46.4 ± 1.7 and 48.2 ± 0.9 yr. The present value was obtained from the specific activity and the radioisotope concentration of several TiO_2 samples, each spiked with a ^{44}Ti activity of about 1.2 μCi. The specific activity was measured via the 1157 keV γ line from the decay of the ^{44}Sc daughter. ^{44}Ti/Ti concentrations were measured with the Argonne FN tandem accelerator in conjunction with an Enge split-pole magnetic spectrograph using the technique of accelerator mass spectrometry. An overall sensitivity of 10^{-10} was achieved which proves accelerator mass spectroscopy to be a powerful tool for radioisotope detection also in a region of rather heavy ion masses. A detailed description of the subtleties of accelerator mass spectroscopy when applied to measure absolute radioisotope concentrations in this heavy mass region is presented.

[RADIOACTIVITY Measured half-life of ^{44}Ti via accelerator mass spectroscopy.]

I. INTRODUCTION

Accelerator mass spectroscopy (AMS) has advanced in recent years to a particularly powerful tool for radioisotope detection.[1-5] Special emphasis has been placed on ultrasensitive isotope detection measurements in terrestrial and/or cosmic probes. In a number of applications[4,5] it has been proven that this technique can be effectively used in answering a variety of cosmic and astrophysical questions of interest and, once the half-life of the investigated radioisotope is sufficiently well known, for more general dating purposes besides the well known ^{14}C dating technique. In a similar way the method allows accurate determination of half-lives for long-lived radioisotopes simply by counting the ions of interest after acceleration and relating this number to the specific activity of the material used in the ion source.[6,7] However, the difficulties of radioisotope identification by means of differential energy loss measurements tend to increase substantially with increasing mass and charge number, A and Z. In addition, the use of complex chemical compounds as injected beams, rather than elemental negative ions, may also severely affect the sensitivity of this method. Molecular ions cannot always be avoided because of constraints in sample preparation and/or negative ion formation. Therefore, by using chemical compounds, nondesired beams from stable isotopes may accidentally match the ion-optical conditions at the low and high energy ends of the accelerator and therefore may pass through the entire system.

In the present application of AMS we have measured the half-life of ^{44}Ti. Apart from rough estimates ranging from 23 to 1000 yr,[8-10] so far only two measurements have been reported in the past, yielding the values 46.4 ± 1.7 yr (Ref. 11) and 48.2 ± 0.9 yr (Ref. 12), with 47.3 ± 0.9 yr as the average number. Both measurements, however, have been carried out under basically the same conditions. The present interest in a remeasurement of the half-life was stimulated by the availability of a substantial amount of ^{44}Ti, which, depending on its half-life, could possibly be used for preparation of a target for future experiments.

II. EXPERIMENTAL PROCEDURE

A. Production and radiochemical separation of ^{44}Ti

^{44}Ti was produced by means of the ^{45}Sc(p,2n) reaction. A high purity ^{45}Sc metal piece of about 2 g/cm^2 areal thickness and 5 g total weight was mounted in a Ta frame and exposed for about 400 h to a 5 μA defocused proton beam of 45 MeV incident energy provided by the Jülich

Isochronous Cyclotron. The energy loss of the proton beam in the Sc material was about 23 MeV; therefore the thick-target yield curve for the (p,2n) reaction was essentially covered. In between the activations γ-ray spectra were taken which showed, apart from the prominent ^{44}Ti decay lines (1499.5, 1157.0, 511, 67.8, and 78.8 keV), strong lines arising from the decay of ^{46}Sc ($T_{1/2}=84$ d; 1120.5 and 889.3 keV). After a period of three years of cooling every short-lived activity had died out. Remaining weak γ lines could be traced back to the decay of ^{172}Hf ($T_{1/2}=1.87$ yr), which was produced by the (p,4n) reaction on ^{175}Lu impurities in the Sc material. The total ^{44}Ti activity obtained was about 200 μCi.

To separate Sc and Ti the activated ^{45}Sc metal was dissolved in a 4M HCl/H_2O_2 solution which was contacted with a solution of bis-2-ethylhexyl ortho-phosphoric acid (HDEDP) and chloroform (1:3) leaving Ti in the aqueous phase and Sc in the organic phase. Traces of Sc in the aqueous phase were removed using a Dowex 50W-X8-400 mesh cation exchange column and eluting Ti with a 1M HCl/H_2O_2 solution. The titanium chloride was then converted to a nitrate and left in a 3M HNO_3 solution.

A small fraction of the Ti solution (~ 5 μCi) was taken for the preparation of samples to be used in the AMS measurements as sputter targets for the inverted Cs-beam sputter source[13] of the Argonne FN tandem accelerator. H_2SO_4 was added and NO_3 was removed. Four different solutions (two with natural Ti isotope concentration and two enriched in ^{48}Ti) were prepared by dissolving TiO_2 material in concentrated H_2SO_4. One of each type was spiked with the ^{44}Ti solution, leaving two blank samples. Possible Sc contaminants were again precipitated with cupferron and the Ti compound was converted to TiO_2. Through this chemical procedure it was found that the purchased enriched $^{48}TiO_2$ material contained a different chemical compound (possibly of tungsten) of about 7% of the original weight.

Six different pellets of 6.4 mm diameter were prepared (two blanks, each containing natural Ti and enriched ^{48}Ti, and four containing natural Ti and enriched ^{48}Ti spiked with ^{44}Ti). Silver powder for thermal and electrical conductivity was added to the carefully weighed amounts of TiO_2. Each pellet contained about 70–80 mg TiO_2 and about 100 mg Ag and was weighed several times to an accuracy of $\pm 0.1\%$, prior to the activity measurement.

B. Activity measurement

The specific γ-ray activity of each pellet was determined with respect to an 8.6 μCi ($\pm 1.9\%$) ^{60}Co calibration source. Once the ^{44}Ti decay is in equilibrium with its daughter ^{44}Sc ($T_{1/2}=3.4$ h), the intensity of the 1157.0 keV γ transition (99.9%) in ^{44}Ca is well suited for a comparison with that of the 1173.2 keV γ line of ^{60}Co, requiring only a very small efficiency correction (1.25%). The specific activity of the pellets was measured with a Ge(Li) detector at a distance of about 100 cm. Self-absorption of the pellets was calculated to have a 1.6% effect. A 0.5% dead-time correction was applied to these measurements owing to the fact that the activity of the ^{60}Co source was higher by about a factor of 7. The statistical error for each of these measurements was about 2.4% superimposed on the 1.9% systematic error owing to the ^{60}Co calibration source. Both natural Ti samples yielded a mean value for the specific activity of 16.07 nCi/mg (TiO_2)$\pm 1.7\%$ (total activity: each ~ 1.2 μCi) and for the ^{48}Ti enriched sample a 7% higher value reflecting the 7% impurity of the purchased ^{48}Ti material as mentioned above.

C. Measurement of the ^{44}Ti/Ti ratio at the tandem accelerator

An overview together with a detailed description of the experimental setup and individual devices used for mass spectrometry at the Argonne FN tandem accelerator has been given in Ref. 14. In Fig. 1 we show a schematic view of the tandem accelerator system together with the Enge split-pole spectrograph as has been used in the present experiment. It should be remembered that the components of the beam transport on the low energy side are—apart from the 40° injection magnet—completely electrostatic, and at the high energy end, completely magnetic.

The basic procedure for radioisotope detection measurements with the system shown in Fig. 1 may be summarized as follows:

(i) The magnetic ion-optical elements at the high energy end are first tuned to optimum beam transport for one stable isotope.

(ii) Once the high energy end is tuned, thus defining a certain magnetic rigidity for the stripped ions, the terminal voltage is changed such that the radioisotope beam under consideration now has the same magnetic rigidity. Accordingly, the 40° injection magnet is set to the radioisotope mass.

Since one is basically operating in a "zero-current" mode, the terminal voltage can no longer be stabilized by the slit current control unit of the 90° analyzing magnet but has to be controlled by a generating voltmeter. The entrance and exit slits of the 90° magnet are opened to allow maximum transmission. To define optimum conditions careful scans of the terminal voltage and the injection magnet current have to be performed.

The change in terminal voltage is one of the most crucial procedures during these measurements and is a potential source of systematic errors. Mainly two effects have to be considered: (i) a change of the focusing properties of the accelerator tubes, and (ii) a change in the charge state distribution after the terminal stripper. For example: A lighter radioisotope mass—compared to its stable counterpart used for normalization—requires a higher terminal voltage to match the high energy magnetic rigidity. This conflicts with the requirement of a lower terminal voltage necessary for equal ion velocities to keep the terminal stripping probabilities constant. In order to minimize such mass fractionation effects it is most favorable to choose a stable isotope for normalization close to the mass of the radioisotope. Mass fractionation effects can be further reduced by choosing the most probable charge state

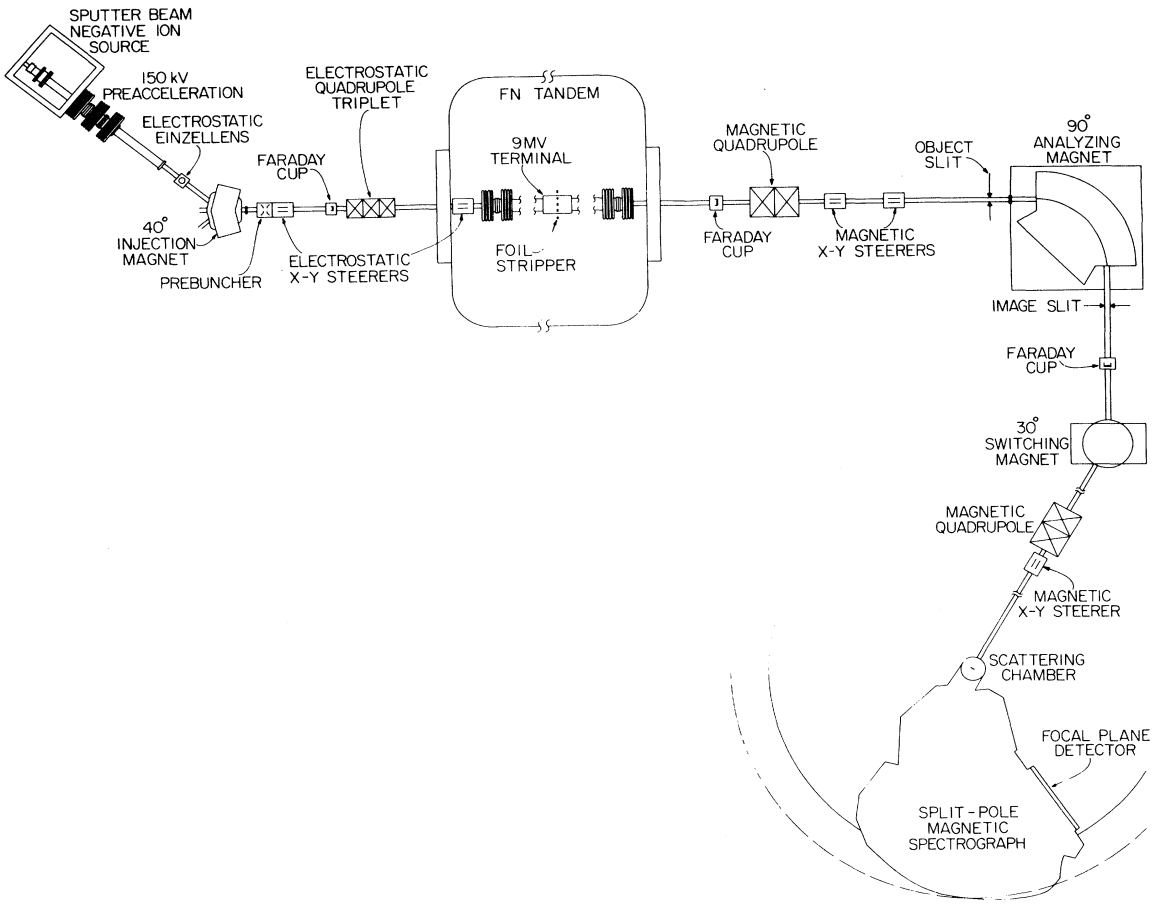

FIG. 1. Schematic view of the beam transport system of the Argonne FN tandem accelerator as it is used for AMS measurements. The low energy part consists of a 40° injection magnet and several electrostatic focusing elements. The components of the high energy end are the 90° analyzing magnet, the 30° switching magnet, two magnetic quadrupoles, and two magnetic x-y steerers. The Faraday cup and the second stripper foil are mounted in the scattering chamber of the Enge split-pole magnetic spectrograph.

at the terminal stripper, rather than choosing one at the steep grade of the charge state distribution curve. The latter condition, however, conflicts with the requirement of higher energy for better Z resolution in the detection system.

One of the major difficulties encountered in AMS measurements is the ever present background beams. Background beams generally arise from various charge exchange processes during acceleration, thus leading to an essentially "white" energy spectrum for various beam components at the exit of the tandem. The completely magnetic high energy beam transport will select appropriate energy and charge state bins, which are ion-optically indistinguishable. These contributions are expected to be considerably enhanced when heavy ions are injected into the accelerator in the form of molecules. Furthermore, the low-energy tails of heavier beams—like those of all stable Ti isotopes in the present experiment—will appreciably contribute to the background beam. The effects may eventually lead to an overall background beam which is several orders of magnitude more intense than the radioisotope beam of interest. The beam degeneracy can be partially removed by introducing a thin foil for charge state dispersion in front of the magnetic spectrograph. With movable shields in front of the focal plane detector one may further select one particular charge state and effectively cut down the background contribution. However, the degeneracy from any beam component having the same charge state as the radioisotope beam under consideration will not be removed. This holds especially for the "white" background beams from the heavier stable isotopes.

The present ^{44}Ti experiment was set up in the following way: A TiO^- beam was injected into the tandem accelerator. At the terminal stripper (carbon foil of 5 $\mu g/cm^2$ thickness) the 9^+ charge state was selected yielding ^{44}Ti ions of 80 MeV total energy. The ^{44}Ti ions then passed through a second stripper foil (50 $\mu g/cm^2$ Au on 10 $\mu g/cm^2$ C) mounted in the target chamber of the Enge split-pole spectrograph. Two movable shields in front of the focal plane detector blocked all but the 15^+ charge state of ^{44}Ti from entering the detector (see, however, below). Two position signals, an energy loss, and a total energy signal were recorded for each event allowing the determination of the ion trajectory as well as an identification of Z and A. It turned out that without physically

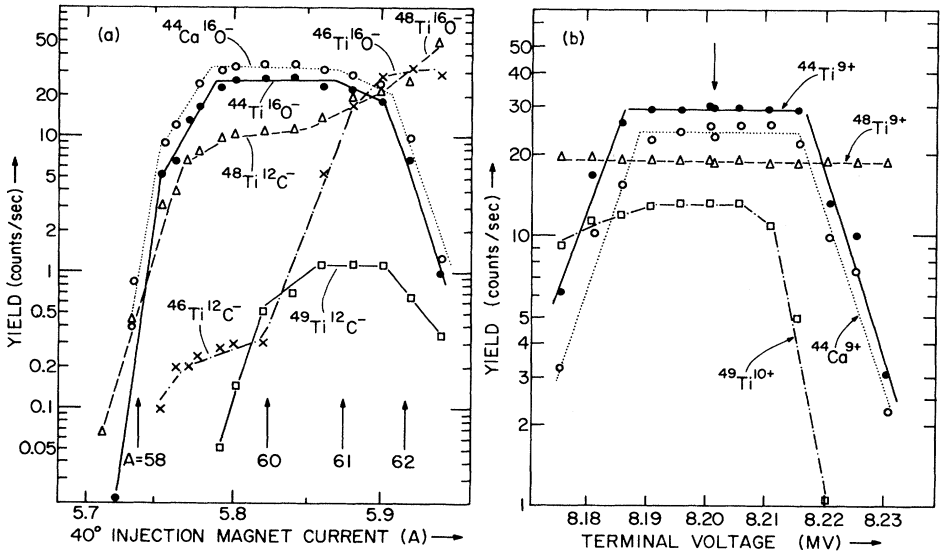

FIG. 2. Results from the beam scanning procedures using the enriched $^{48}TiO_2$ sample. All lines are drawn to guide the eye. (a) Scan of the 40° injection magnet current in the mass range $A \simeq 58-62$. At this stage the terminal voltage was set at 8.215 MV, which is slightly off the optimum value for ^{44}Ti detection. Note that two different molecular species are observed for ^{46}Ti and ^{48}Ti. (b) Scan of the terminal voltage for various ions accepted by the high energy beam transport system, once the injection magnet is set to inject mass 60. The profile from the degenerate $^{49}Ti^{10+}$ ions injected as $^{49}Ti^{12}C^-$ is also included. The arrow marks the working condition for ^{44}Ti detection.

shielding the focal plane detector the count rate would have been intolerably high. When using the natural samples as sputter targets a measurable beam current in the low picoampere range was observed at the Faraday cup inside the scattering chamber, even when the terminal voltage was set for ^{44}Ti. This situation was in fact not expected and was found to be owing to a degenerate beam of $^{49}Ti^{10+}$, which, injected as $^{49}Ti^{12}C^-$, happened to match almost exactly the rigidity condition at the high energy end. The source pellets did not contain carbon, but carbon is an abundant contaminant in the source. As the two degenerate beams have different charge states ($^{44}Ti^{9+}$,$^{49}Ti^{10+}$), this degeneracy is in principle removed after passing through the second stripper foil in the spectrograph target chamber. In this special case, however, the 16^+, 17^+, 18^+, and 19^+ charge states of ^{44}Ti again turn out to be almost degenerate to the 18^+, 19^+, 20^+, and 21^+ charge states of ^{49}Ti, thus leaving only the lower charge states for an identification of ^{44}Ti.

The injection of a considerable TiC^- beam was discovered during the scanning procedure of the 40° injection magnet and the terminal voltage. This procedure is used to find the optimum beam transport conditions for the ^{44}Ti ions measured in the spectrograph. Simultaneously, valuable information about background beams is obtained. In Fig. 2 the results of the scans are shown, where we used the ^{48}Ti enriched sample in order to achieve cleaner conditions. Plotted are the counting rates of the respective particle groups as observed in the focal plane detector. The 40° magnet scan [Fig. 2(a)] shows the profile of ^{44}Ti and that of its isobar ^{44}Ca (which is also a source contaminant), both injected as oxides at mass 60. The scan also shows that the mass acceptance in this region is about ± 2 mass units, therefore slight changes or minor drifts of the 40° magnet will not affect the overall transmission. In addition, two different background components of ^{48}Ti are identified. At mass 60 ^{48}Ti is injected as $^{48}TiC^-$, whereas at higher masses $^{48}TiO^-$ significantly starts to contribute to a general background beam. A similar behavior is observed for ^{46}Ti, but at a lower level owing to its low concentration in the enriched sample, although the ^{46}Ti yield is considerably enhanced over ^{48}Ti relative to what is expected from the ^{48}Ti/^{46}Ti isotope ratio, due to its proximity to ^{44}Ti.

In Fig. 2(b) a similar scan of the terminal voltage is shown. The width of the beam profile turns out to be 30 kV, which corresponds to an acceptance for the 90° analyzing magnet of about 290 keV. This rather large value primarily results from the wide opening of the entrance and exit slits. In this figure [2(b)] one also notices that the ^{48}Ti beam component is essentially "white" without showing any dependence on the terminal voltage.

Although the ^{49}Ti contribution seems to be at a rather low level, it is, even for the ^{48}Ti enriched sample, the strongest beam component reaching the spectrograph. Injected as a carbide [cf. Fig. 2(a)] and stripped to the 10^+ charge state, $^{49}Ti^{10+}$ is nearly a tuned beam. This is demonstrated by the beamlike profile in the terminal voltage scan [Fig. 2(b)]. The slight shift of about 15 kV observed with respect to the $A=44$ beam is just the value one expects from the slight difference in magnetic rigidity. The ^{49}Ti component was in fact observed by accident:

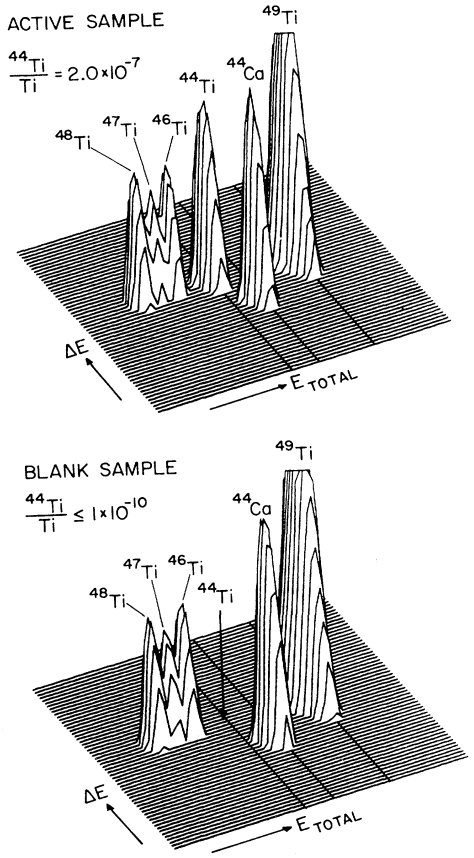

FIG. 3. An isometric view of the two-dimensional ΔE-E spectrum for the $Z \simeq 22$ region measured with the focal plane detector of the magnetic spectrograph. All scales are linear. The lower part shows the results from a blank sample whereas the upper part was obtained using a ^{44}Ti spiked sample. The different isotopes are indicated. All ions except ^{49}Ti are identified as being in the 15^+ charge state. The strong beamlike ^{49}Ti component accidentally passed through in the 20^+ charge state (see the text).

The movable shields set to select the 15^+ charge state of ^{44}Ti opened up slightly at the low energy end and allowed the 20^+ charge state of the $^{49}Ti^{10+}$ beam to leak into the focal plane detector. By taking into account the low isotopic abundance of ^{49}Ti in the enriched sputter target as well as the low probability for a 20^+ charge state production after second stripping, one calculates a beam current for the natural sample of several picoamperes, which well compares to the measured value in front of the spectrograph. The disentangling of the ^{49}Ti component may be regarded as an instructive example for the analytic power of the AMS technique. It should also be pointed out that a complete knowledge of all existing beam components is essential since unexpected beams may also affect the beam current measurements when switching to the stable isotope. This is especially true for the isotope ^{48}Ti. Injected as $^{48}Ti^{16}O^-$, the $^{48}Ti^{9+}$ beam is completely degenerate with the $^{16}O^{3+}$ component, which hence obscures the $^{48}Ti^{9+}$ current measurement. ^{48}Ti could therefore not be used for normalization.

Knowing the operating conditions of the system, ten different concentration measurements were carried out using both spiked samples with the natural isotopic abundances. Before and after each measurement the beam current of ^{46}Ti was measured using the Faraday cup mounted in the spectrograph scattering chamber. Charge losses due to secondary electron emission were avoided by a suppressor ring at -300 V supplied by a battery. The charge integrator was carefully calibrated to $\leq 1\%$ by means of a picoampere source that provided a constant dV/dt capicator discharge current. The $^{46}Ti^{9+}$ beam current was typically of the order of 100 pA, and the counting rate of ^{44}Ti ions was of the order of 50 counts/sec for the 15^+ charge state. From these values one obtains ^{44}Ti/Ti ratios of about 2×10^{-7}. Each run took about 15 min, during which no sudden beam bursts were observed. To guard against loss of counts, data acquisition was gated off whenever the terminal voltage fluctuations exceeded ± 2 kV.

A typical ΔE-E spectrum obtained during the measurements is shown in Fig. 3 for the $Z \approx 22$ region. The upper spectrum shows the yield from a ^{44}Ti spiked sample, whereas the lower spectrum was obtained with a blank sample. It may be noted that owing to different energy losses in the entrance foil of the focal plane detector the isobars ^{44}Ti and ^{44}Ca have a slightly different residual energy, which further helps to separate them.

The selection of only one charge state in the focal plane detector requires a measurement of the charge state distribution. Because of the partial degeneracy with ^{49}Ti, as mentioned above, the charge state distribution of ^{44}Ti could not be measured directly. Instead we used a ^{46}Ti beam of equal velocity at the second stripper foil and counted the Coulomb-scattered ions at 5° laboratory angle. Since the charge state distribution only depends on the projectile's atomic number and velocity, the measured values correspond to the ^{44}Ti charge state distribution. The results are summarized in Table I.

D. Mass fractionation effects

The effects of mass fractionation during acceleration are a potential source of systematic errors. Mass fractionation effects are primarily induced by different focusing conditions of the accelerator tubes as a function of the terminal voltage, and different charge state production probabilities in the terminal stripper foil as a function of the ion velocity. Both effects are expected to contribute in this experiment, since the high energy magnetic rigidity for the respective ion beams is kept constant. In order to separate these effects we proceeded in the following way: The beam currents of the different stable isotopes relative to their isotopic abundance in the sputter target were first measured for constant ion velocity at the terminal stripper. This measurement reveals the mass dependence of the focusing conditions of the tubes (and/or mass-dependent sputter yields which might also be conceivable). The results are shown in Fig. 4, where the average

TABLE I. Measured charge state distribution for 83.8 MeV ^{46}Ti ions (which correspond to 80.1 MeV ^{44}Ti ions) after passing through a 50 μg/cm^2 Au foil evaporated on a 10 μg/cm^2 carbon foil. A 0.25% probability for the nonmeasured charge states $n \leq 11$ and $n \geq 20$ has been assumed.

Charge state	12	13	14	15	16	17	18	19
Probability (%)	1.59	7.73	20.15	28.51	24.85	12.72	3.65	0.53
Error (% of probability value)	3.8	1.3	<1.	<1.	<1.	<1.	1.5	4.7

currents of a series of three different runs are plotted. For each measured point the low and high energy ends were completely retuned in a consistent way. A terminal voltage dependent increase in the relative yields is observed, which in subsequent analyses has been approximated by a linear dependence. For the present experiment equal rigidity for ^{46}Ti and ^{44}Ti at the high energy end corresponds to terminal voltage settings of 7.835 MV (^{46}Ti) and 8.203 MV (^{44}Ti), resulting, for the ^{44}Ti yield, in a terminal voltage dependent enhancement factor of 1.071 (±0.023). An equal velocity at the terminal stripper, however, corresponds to a voltage setting for ^{46}Ti of about 8.5 MV. This data point has been added in Fig. 4 and a further enhancement for the ^{44}Ti output of 1.130 (±0.028) is deduced. This value agrees fairly well with an estimate using the empirical formula for charge state production probabilities of Ref. 15. Both effects produce an overall enhancement factor of 1.210 (±0.0275) which defines the total mass fractionation. Unfortunately a data point for ^{48}Ti is not available since the ^{48}Ti^{9+} beam is degenerate with the ^{16}O^{3+} beam as mentioned above.

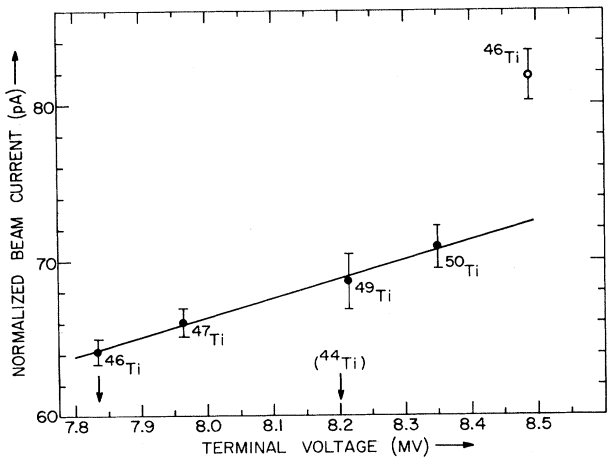

FIG. 4. Measurement of the mass fractionation for various Ti isotopes (injected as TiO$^-$) as a function of the terminal voltage. The full circles denote the measured beam currents after the 90° analyzing magnet for the respective isotopes having equal velocities at the terminal stripper. The current is normalized to the respective isotopic abundance, and the line represents a linear fit to the data points. The arrows indicate the terminal voltage settings for the ^{44}Ti and ^{46}Ti measurements. The open circle data point reflects, in addition, the velocity dependence of the charge state distribution (see the text).

It should be pointed out that the correction for mass fractionation strongly depends on having accurate values for the natural isotopic abundances. These quantities are not always known to the desired accuracy and sometimes may even differ depending on the origin of a natural sample. In the present situation we used the values from Ref. 16 (^{46}Ti, 8.012%; ^{47}Ti, 7.331%; ^{48}Ti, 73.814%; ^{49}Ti, 5.497%; ^{50}Ti, 5.346%), which seem to be the most accurate values presently available for the Ti isotopes.

III. RESULTS AND DISCUSSION

For the present experimental setup the half-life of ^{44}Ti is expressed by the following equation (derived from the basic law of radioactive decay, $dN/dt = -\lambda N$):

$$T_{1/2}(\mathrm{yr}) = 6.454\times10^{-3}\frac{m(\mathrm{TiO_2})}{A(^{44}\mathrm{Ti})}\frac{N(^{44}\mathrm{Ti}^{15+})}{I(^{46}\mathrm{Ti}^{9+})} \times p(^{46}\mathrm{Ti})\frac{1}{W(15^+)}\frac{1}{f},$$

where $A(^{44}\mathrm{Ti})/m(\mathrm{TiO_2})$ is the specific activity in μCi/mg of the sample used as a sputter target, $N(^{44}\mathrm{Ti}^{15+})$ is the counting rate of ^{44}Ti ions in the focal plane detector after stripping to a 15^+ charge state, $I(^{46}\mathrm{Ti}^{9+})$ is the beam current of the ^{46}Ti^{9+} ions in charge nA, $p(^{46}\mathrm{Ti})$ is the iso-

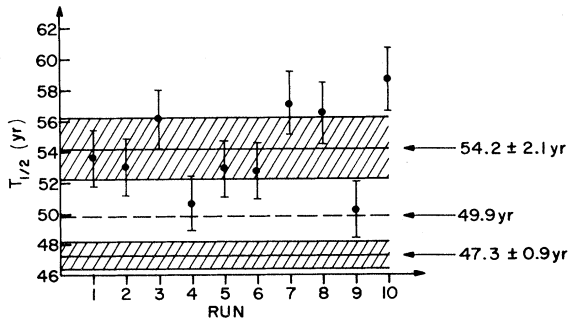

FIG. 5. The results of ten different half-life measurements, with a mean value of 54.2±2.1 yr. The mean of the previously reported values (Refs. 11 and 12) is indicated by the hatched area around 47.3 yr, whereas the value obtained after applying a small correction to this number (cf. the text) is indicated by the dashed line.

topic abundance of ^{46}Ti in the sample, $W(15^+)$ is the 15^+ charge state probability of ^{44}Ti after passing through the second stripper foil, and f is the total mass fractionation factor.

In Fig. 5 the results are plotted for all ten measurements. The error bars reflect the total error arising from different sources, i.e., the statistical error from the activity measurement, the systematic error from the ^{60}Co calibration source, and the errors related to the mass fractionation and charge state distribution measurements. The statistical errors from the ion counting rate in the spectrograph are comparatively small. Deviations are still present, possibly pointing to small fluctuations in the ion source output or in the overall transmission from the ion source to the detector. The mean value for the half-life is 54.2 ± 2.1 yr. The error is obtained by adding in quadrature the systematic error and the mean deviation.

Our value for the half-life of ^{44}Ti is higher than the previously accepted value of 47.3 yr. However, it should be noted that in the previous measurements the β^+ decay of the ^{44}Sc daughter product has been used for the activity measurements and compared to a ^{22}Na standard. The branching ratios of both ^{44}Sc and ^{22}Na, as well as the half-life of ^{22}Na, have been subject to small changes in the past. In view of the new values[17] as well as a slightly different ^{46}Ti/^{48}Ti isotopic ratio used in our measurement, the previously measured value will increase to 49.9 yr, which then lies at the lower limit of the present measurement.

The present measurement has confirmed the short half-life of ^{44}Ti. Although ^{44}Ti may only be of limited use for dating experiments, the present work proves AMS to be effectively applicable for medium heavy mass radioisotopes, even under rather complex conditions. For higher precision measurements of half-lives other methods may eventually be favored. However, the advantages of AMS clearly lie in the ultrasensitive concentration measurements covering a region hardly accessible with other methods. The present sensitivity was of the order of 10^{-10} and it is conceivable that by adding a Wien filter or an electrostatic separator to the existing beam transport system one could substantially increase the overall sensitivity for medium weight radioisotope concentration measurements. In addition, an order of magnitude increase of the TiO^- beam should also be feasible with an improved ion source, which further increases the sensitivity.

ACKNOWLEDGMENTS

We would like to thank K. J. Jensen for the chemical preparation of the TiO_2 samples and C. M. Stevens for valuable discussions on spectrometric details. This work was supported in part by the U. S. Department of Energy under Contract W-31-109-Eng-38. One of the authors (D.F.) acknowledges the financial support of the Deutsche Forschungsgemeinschaft.

[1]K. H. Purser, A. E. Litherland, and H. E. Gove, Nucl. Instrum. Methods 162, 637 (1979).
[2]T. S. Mast and R. A. Muller, Nucl. Sci. Appl. 1, 7 (1980).
[3]A. E. Litherland, Annu. Rev. Nucl. Part. Sci. 30, 437 (1980).
[4]Proceedings of the Symposium on Accelerator Mass Spectroscopy, Argonne, 1981, Argonne National Laboratory Report ANL/PHY-81-1, 1981, edited by W. Henning, W. Kutschera, R. K. Smither, and J. L. Yntema.
[5]M. Stuiver and R. S. Kra, Radiocarbon (to be published).
[6]W. Kutschera, W. Henning, M. Paul, R. K. Smither, E. J. Stephenson, J. L. Yntema, D. E. Alburger, J. B. Cumming, and G. Harbottle, Phys. Rev. Lett. 45, 592 (1980).
[7]D. Elmore, N. Anantaraman, H. W. Fulbright, H. E. Gove, H. S. Hans, K. Nishiizumi, M. T. Murell, and M. Honda, Phys. Rev. Lett. 45, 589 (1980).
[8]R. A. Sharp and R. M. Diamond, Phys. Rev. 93, 358 (1954); 96, 1713 (1954).
[9]J. R. Huizenga and J. Wing, Phys. Rev. 106, 90 (1957).
[10]M. Honda and D. Lal, Nucl. Phys. 51, 363 (1964).
[11]J. Wing, M. A. Wahlgren, C. M. Stevens, and K. A. Orlandini, J. Inorg. Nucl. Chem. 27, 487 (1965).
[12]P. E. Moreland, Jr., and D. Heymann, J. Inorg. Nucl. Chem. 27, 493 (1965).
[13]P. J. Billquist and J. L. Yntema, Nucl. Instrum. Methods 178, 9 (1980).
[14]W. Henning, W. Kutschera, M. Paul, R. K. Smither, E. J. Stephenson, and J. L. Yntema, Nucl. Instrum. Methods 184, 247 (1981).
[15]R. O. Sayer, Rev. Phys. Appl. 12, 1543 (1977).
[16]F. R. Niederer, D. A. Papanastassiou, and G. J. Wasserburg, Geochim. Cosmochim. Acta 45, 1017 (1981).
[17]*Table of Isotopes*, 7th ed., edited by C. M. Lederer and V. S. Shirley (Wiley, New York, 1978).